Structure of molecular liquids: Closure relations for hard spheroids

David L. Cheung,[1,*] Lucian Anton,[2,3,†] Michael P. Allen,[1,‡] and Andrew J. Masters[2,§]
[1]*Department of Physics and Centre for Scientific Computing, University of Warwick, Coventry, CV4 7AL, United Kingdom*
[2]*School of Chemical Engineering and Analytical Science, University of Manchester, Sackville Street, Manchester, M60 1QD, United Kingdom*
[3]*Institute of Atomic Physics, INFLPR, Lab 22, P.O. Box MG-36 R76900, Bucharest, Romania*
(Received 20 June 2007; published 8 October 2007)

We present the results of Monte Carlo simulations of hard spheroids of revolution of different elongations. Both prolate and oblate shapes are examined. A systematic study of the bridge function $b(1,2)$, and direct comparison with the indirect correlation function $\gamma(1,2)=h(1,2)-c(1,2)$ at densities spanning the isotropic fluid range, allow us to evaluate the accuracy of various proposed closure relations for integral equations.

DOI: 10.1103/PhysRevE.76.041201 PACS number(s): 61.20.Gy, 61.20.Ja, 05.20.Jj

I. INTRODUCTION

Theory and simulation have revealed a great deal about the thermodynamic properties and fluid structure of homogeneous fluids of spherical particles [1,2]. Simulation has been used to calculate the total and direct correlation functions [3], the cavity function [4,5], and the bridge function [6–8]. On the theoretical side, integral equation theory (IET) is now capable of making some very accurate predictions. The Percus-Yevick (PY) and hypernetted chain (HNC) theories have now been extended, for example, by mixing closures so as to obtain identical virial and compressibility equations of state [9,10]. An alternative approach has been to incorporate approximate forms for the bridge function in the HNC closure [11–13].

The equilibrium properties of isotropic fluids of nonspherical particles are less well characterized. The PY and HNC equations have been solved for axially symmetric particles (e.g., hard spheroids, hard spherocylinders, and truncated hard spheres) and the general conclusion is that the HNC is superior to the PY method for significantly aspherical particles, but that there is still a substantial discrepancy between theory and simulation, especially at high density [14–17]. Singh *et al.* [18] applied a nonspherical version of the Rogers-Young method of mixing PY and HNC closures, obtaining results for spheroids in good agreement with simulation. A series of papers [19–23] has investigated the use of a modified Verlet-bridge closure, reporting improved results. With the exception of the pioneering study of Lomba *et al.* [24] on hard diatomic molecules, there have been no direct determinations of the bridge function for nonspherical systems. Consequently, our understanding of these systems is still not as complete as in the case of spherical particles, and a systematic study of pair structure as a function of molecular shape and density is sorely needed.

In a previous paper [25] we presented methodologies for calculating the direct correlation and cavity and bridge functions for isotropic fluids of axially symmetric particles using advanced the Monte Carlo (MC) techniques. These methods were used to calculate the molecular correlation functions for a fluid of hard spheroids with major axis of length A and minor axis of length B, with elongation $e=A/B=3$, over a range of densities in the isotropic phase. Comparisons were made with IET, and with a virial expansion of the bridge function. In the present paper we greatly extend this study, to encompass elongations $e=\frac{3}{2},2,3,5$ and their inverses. We concentrate on the bridge function itself, and the information that can be obtained about possible closure relations.

The paper is organized as follows. Section II defines the bridge function and relates it to the integral equations that arise from applying closure relations to the Ornstein-Zernike equation. Section III contains a brief description of the computational methods used in this work. Results are presented in Sec. IV and conclusions in Sec. V.

II. CLOSURE RELATIONS AND SPHERICAL HARMONIC EXPANSIONS

The Ornstein-Zernike equation for a homogeneous fluid of axially symmetric molecules is [1,2]

$$h(1,2)=c(1,2)+\frac{\rho}{4\pi}\int d3\, c(1,3)h(3,2). \tag{1}$$

Here $h(1,2)=g(1,2)-1$ is the total correlation function, $g(1,2)$ the pair distribution function, $c(1,2)$ the direct correlation function, and ρ the number density. We have abbreviated $(\boldsymbol{r}_i,\boldsymbol{u}_i)\rightarrow i$, where $\boldsymbol{r}_i$ denotes the center-of-mass position, and $\boldsymbol{u}_i$ a unit vector along the symmetry axis, of particle i.

To determine $h(1,2)$ and $c(1,2)$, Eq. (1) is usually supplemented by an approximate closure relation. The exact closure relation can be written as follows [1]:

$$y(1,2)\equiv g(1,2)\exp[V(1,2)/k_{\mathrm{B}}T]=\exp[\gamma(1,2)+b(1,2)], \tag{2}$$

where $y(1,2)$ is the cavity or background correlation function, $V(1,2)$ is the intermolecular pair potential, T is the temperature, k_{B} is Boltzmann's constant, $\gamma(1,2)=h(1,2)-c(1,2)$, and $b(1,2)$ is the bridge function. Equation (2) may

*david.cheung@warwick.ac.uk
†lucian.anton@manchester.ac.uk
‡m.p.allen@warwick.ac.uk
§andrew.masters@manchester.ac.uk

be regarded as a definition of $b(1,2)$. The approximate closure relations may be regarded as approximations to the unknown $b(1,2)$. In particular, the best-known closures [1,2] are as follows.

Hypernetted chain. $b^{\mathrm{HNC}}(1,2)=0$.

Percus-Yevick. $b^{\mathrm{PY}}(1,2)=-\gamma(1,2)+\ln[1+\gamma(1,2)]$.

A set of more sophisticated closure relations are based on the form introduced by Verlet [26],

$$b(1,2)=-\frac{\frac{1}{2}\gamma(1,2)^2}{1+\alpha\gamma(1,2)}. \tag{3}$$

Different choices of the parameter α in Eq. (3) correspond to the following closures.

Verlet bridge (VB). $b^{\mathrm{VB}}(1,2)$, Eq. (3) with $\alpha=0.8$ [26].

Modified Verlet bridge (MV). $b^{\mathrm{MV}}(1,2)$, Eq. (3) with $\alpha=1.1-(2/\pi)\eta$ [19,23].

Henderson-Chan-Degrève (HCD). $b^{\mathrm{HCD}}(1,2)$, Eq. (3) with

$$\alpha=\frac{17}{120\eta}+0.515-0.2210\eta, \tag{4}$$

where η is the packing fraction [27,28]. The above closures were all originally proposed for hard-sphere systems, but are easily extended to nonspherical hard particles; for hard spheroids $\eta=(\pi/6)\rho AB^2$.

The numerical solution of the integral equation and MC calculations of $b(1,2)$ are based upon the expansion of two-particle functions in a basis set of rotational invariants [2,29]

$$F(1,2)=\sum_{mn\ell}F^{mn\ell}(r)\Phi^{mn\ell}(\boldsymbol{u}_1,\boldsymbol{u}_2,\hat{\boldsymbol{r}}), \tag{5}$$

$$\Phi^{mn\ell}(\boldsymbol{u}_1,\boldsymbol{u}_2,\hat{\boldsymbol{r}})=4\pi\sum_{\mu\nu\lambda}\begin{pmatrix} m & n & \ell \\ \mu & \nu & \lambda \end{pmatrix}Y_{m\mu}(\boldsymbol{u}_1)Y_{n\nu}(\boldsymbol{u}_2)\sqrt{\frac{4\pi}{2\ell+1}}Y_{\ell\lambda}(\hat{\boldsymbol{r}}), \tag{6}$$

where r is the intermolecular distance. All the vectors are expressed in an arbitrary "laboratory frame:" $\hat{\boldsymbol{r}}$ is a unit vector pointing along the line of centers, and $\boldsymbol{u}_1,\boldsymbol{u}_2$ are the orientations of the molecules. $Y_{m\chi}(\boldsymbol{u})$ are the spherical harmonic functions, and $\left(\begin{smallmatrix} m & n & \ell \\ \mu & \nu & \lambda \end{smallmatrix}\right)$ is the standard $3j$ symbol.

Some quantities of interest are easier to compute in a system of coordinates whose z axis lies along the intermolecular vector: the "molecular frame." With vectors $\tilde{\boldsymbol{u}}$ referred to this frame, the expansion has the form

$$F(1,2)=4\pi\sum_{mn\chi}F_{mn\chi}(r)Y_{m\chi}(\tilde{\boldsymbol{u}}_1)Y_{n\bar{\chi}}(\tilde{\boldsymbol{u}}_2), \tag{7}$$

where $\bar{\chi}=-\chi$. The two sets of coefficients are connected through the χ transform and its inverse:

$$F_{mn\chi}(r)=\sum_{\ell}\begin{pmatrix} m & n & \ell \\ \chi & \bar{\chi} & 0 \end{pmatrix}F^{mn\ell}(r), \tag{8a}$$

TABLE I. Orientations of molecules relative to the center-center vector, used in the Duh-Haymet plots.

Angle (deg)	Orientation							
	e	s	t	x	a	b	c	d
ϕ	0	0	0	90	0	60	120	180
θ_1	0	90	0	90	45	45	45	45
θ_2	0	90	90	90	45	45	45	45

$$F^{mn\ell}(r)=(2\ell+1)\sum_{\chi}\begin{pmatrix} m & n & \ell \\ \chi & \bar{\chi} & 0 \end{pmatrix}F_{mn\chi}(r). \tag{8b}$$

III. COMPUTATIONAL METHODS

The simulations, the techniques used to invert the data and extract the bridge functions, and the method used to solve the integral equations subject to given closure relations, were described in detail in Ref. [25]. Therefore, only a brief summary will be given here.

Standard constant-*NVT* Monte Carlo simulation methods were employed. Spherical harmonic expansion coefficients of the pair distribution function $g(1,2)$ and hence $h(1,2)$ were computed, using system sizes of $N=2048$ molecules, and run lengths (after equilibration) of 5×10^5 MC sweeps (each sweep is on average one attempted translation and one attempted rotation per molecule). From $h(1,2)$, the direct correlation function $c(1,2)$ was obtained by inverting the Ornstein-Zernike equation (1). Spherical harmonic expansions were truncated at $m_{\max}=n_{\max}=8$ and the grid spacing was $\delta r=0.01B$. The cavity correlation function $y(1,2)$ was calculated using a smaller system size, $N=512$ molecules. Special sampling techniques were used [25], and the bridge function $b(1,2)$ was obtained by inverting the closure relation (2).

To solve the integral equations we have used the general approach of Refs. [15,30], calculating the solution by expansion in rotational invariants of the correlation functions, Eq. (5); the expansions are truncated at $m_{\max}=n_{\max}=8$ and all nonzero components consistent with this truncation are kept. The integral equation was discretized on a grid in steps of $\delta r=0.01B$ for the prolate shapes, and $\delta r=0.005B$ for the oblate shapes. The resulting system of nonlinear equations is solved using the Newton iterative solver presented in Ref. [31].

Results are presented here for the eight elongations $e=5,3,2,\frac{3}{2},\frac{2}{3},\frac{1}{2},\frac{1}{3},\frac{1}{5}$, at reduced densities $\rho^*=\rho AB^2/\sqrt{2}=0.1,0.2,0.3,0.4,0.5,0.6$, except that the highest two densities are omitted for $e=5,\frac{1}{5}$. (In these units, $\rho^*=1$ corresponds to the density of regular close packing based on the fcc or hcp structure; in passing we note that regular crystal structures of higher density exist [32,33].) Simulations were also performed at $e=1.1$ and $1/1.1$ for comparison with the results of hard spheres, and for $\rho^*=0.7$ at elongations $e=2,\frac{1}{2}$, but these are not reported in detail here.

For convenience later, we list in Table I eight relative

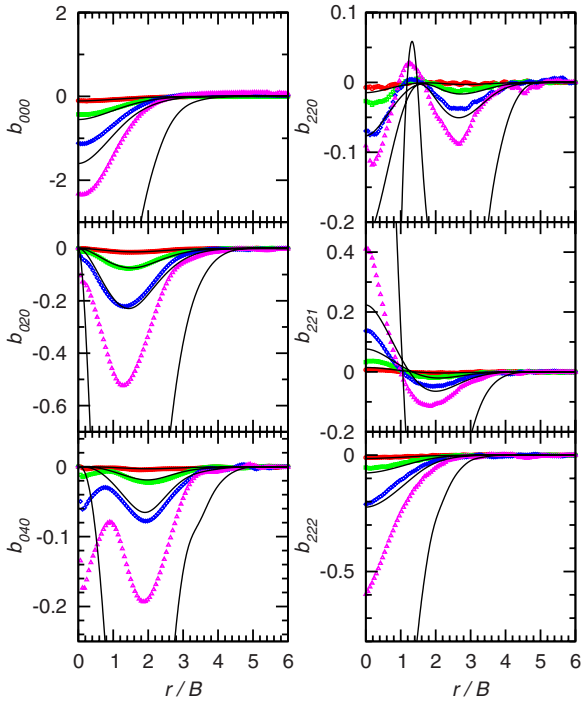

FIG. 1. (Color online) Spherical harmonic coefficients of the bridge function in the molecular frame, $b_{mn\chi}(r)$, determined by Monte Carlo simulation, for prolate spheroids of elongation $e=A/B=5$. Densities: $\rho^*=0.1$ (circles, red), 0.2 (squares, green), 0.3 (diamonds, blue), 0.4 (triangles, magenta). The solid lines are the corresponding results $b_{mn\chi}^{\mathrm{HCD}}(r)$ of solving the Ornstein-Zernike equation with the Henderson-Chan-Degrève [27,28] modified Verlet-bridge closure.

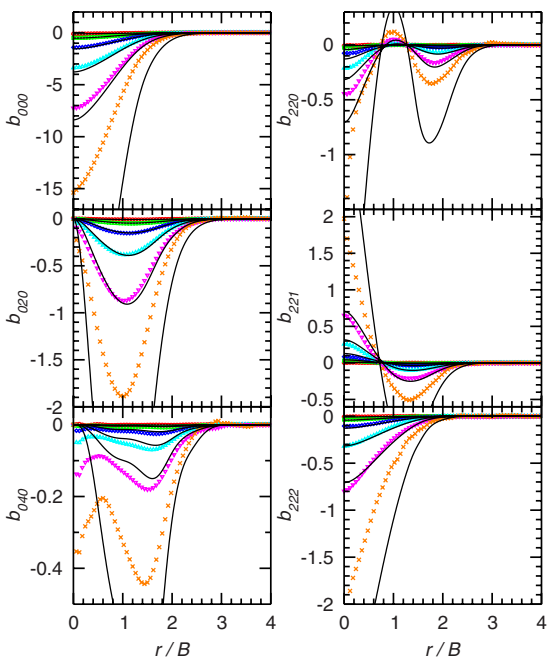

FIG. 3. (Color online) Spherical harmonic coefficients of the bridge function in the molecular frame, $b_{mn\chi}(r)$, determined by Monte Carlo simulation, for prolate spheroids of elongation $e=A/B=3$. Densities: $\rho^*=0.1$ (circles, red), 0.2 (squares, green), 0.3 (diamonds, blue), 0.4 (triangles, cyan), 0.5 (inverted triangles, magenta), 0.6 (crosses, orange). The solid lines are the corresponding results $b_{mn\chi}^{\mathrm{HCD}}(r)$ of solving the Ornstein-Zernike equation with the HCD modified Verlet-bridge closure.

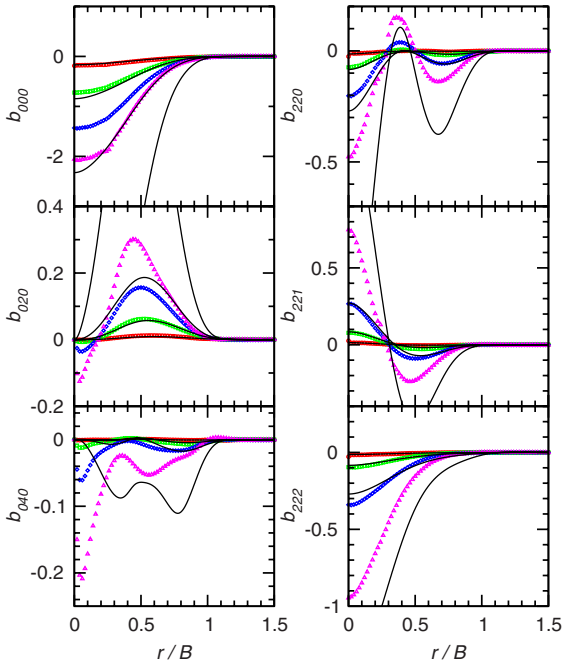

FIG. 2. (Color online) Spherical harmonic coefficients of the bridge function in the molecular frame, $b_{mn\chi}(r)$, determined by Monte Carlo and integral equation theory using the modified HCD Verlet-bridge closure, for oblate spheroids of elongation $e=A/B=1/5$. Notation as for Fig. 1.

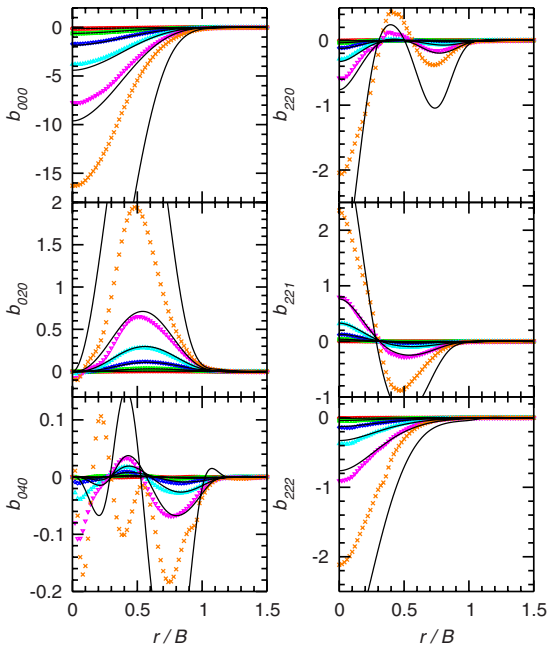

FIG. 4. (Color online) Spherical harmonic coefficients of the bridge function in the molecular frame, $b_{mn\chi}(r)$, determined by Monte Carlo and integral equation theory using the HCD modified Verlet-bridge closure, for oblate spheroids of elongation $e=A/B=1/3$. Notation as for Fig. 3.

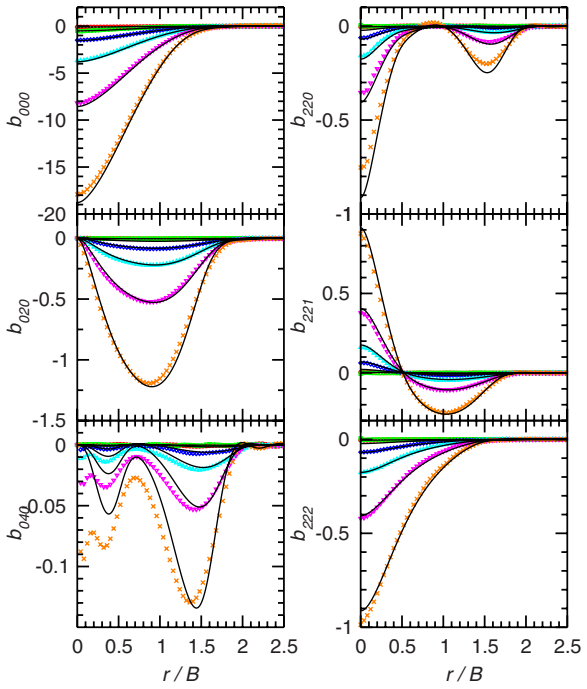

FIG. 5. (Color online) Spherical harmonic coefficients of the bridge function in the molecular frame, $b_{mn\chi}(r)$, determined by Monte Carlo and integral equation theory using the HCD modified Verlet-bridge closure, for prolate spheroids of elongation $e=A/B=2$. Notation as for Fig. 3.

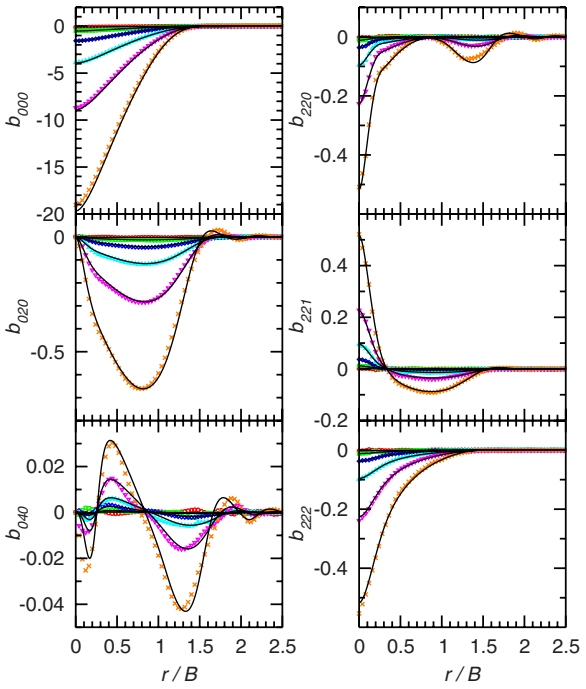

FIG. 7. (Color online) Spherical harmonic coefficients of the bridge function in the molecular frame, $b_{mn\chi}(r)$, determined by Monte Carlo and integral equation theory using the HCD modified Verlet-bridge closure, for prolate spheroids of elongation $e=A/B=3/2$. Notation as for Fig. 3.

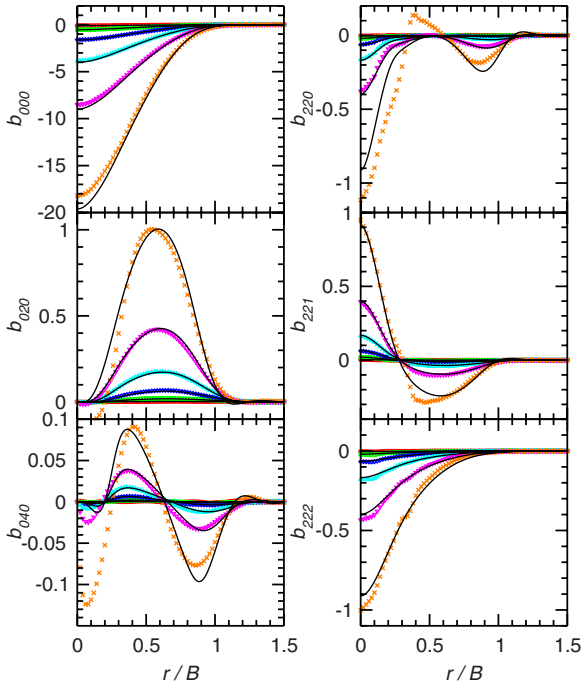

FIG. 6. (Color online) Spherical harmonic coefficients of the bridge function in the molecular frame, $b_{mn\chi}(r)$, determined by Monte Carlo and integral equation theory using the HCD modified Verlet-bridge closure, for oblate spheroids of elongation $e=A/B=1/2$. Notation as for Fig. 3.

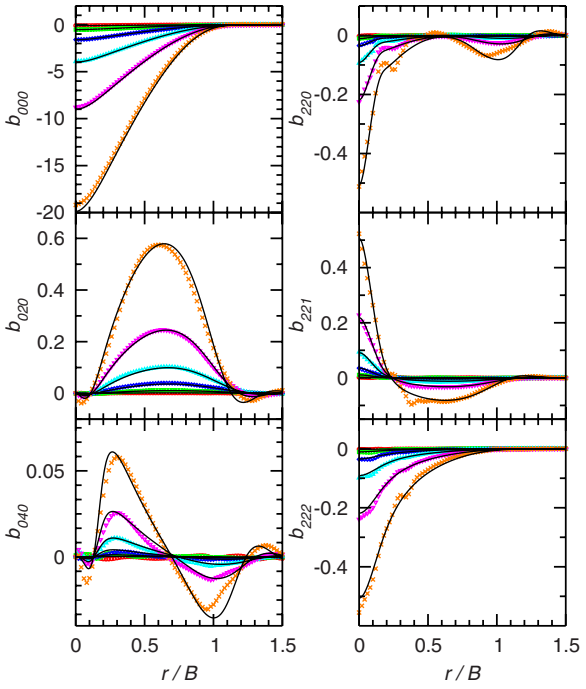

FIG. 8. (Color online) Spherical harmonic coefficients of the bridge function in the molecular frame, $b_{mn\chi}(r)$, determined by Monte Carlo and integral equation theory using the HCD modified Verlet-bridge closure, for oblate spheroids of elongation $e=A/B=2/3$. Notation as for Fig. 3.

arrangements of pairs of linear molecules. For convenience they are referred to by a single letter. The relative orientation angles are defined by $\cos\theta_1=\boldsymbol{u}_1\cdot\hat{\boldsymbol{r}}$, $\cos\theta_2=\boldsymbol{u}_2\cdot\hat{\boldsymbol{r}}$, and $\cos\phi=\hat{\boldsymbol{p}}_1\cdot\hat{\boldsymbol{p}}_2$ where $\hat{\boldsymbol{p}}_i$ is the unit vector in the direction $\boldsymbol{p}_i=\boldsymbol{u}_i\times\hat{\boldsymbol{r}}$. Orientation "e" corresponds to an end-to-end arrangement; "s" is side by side; "t" is a T shape; "x" is a crossed arrangement where the molecular axes and the center-center vector are all mutually perpendicular. The remaining orientations "a"–"d" are less symmetrical: both molecules are tilted at 45° relative to the center-center vector, and four different twist angles ϕ are chosen.

IV. RESULTS

A. Angular components of the bridge function

In Figs. 1–8 we present several spherical harmonic components of the bridge function $b_{mn\chi}(r)$, computed in the molecular frame from the Monte Carlo simulations, for both prolate and oblate spheroids. The results are compared with the predictions of integral equation theory using the HCD modified Verlet-bridge closure [27,28], which we find to be the best approximation to the bridge function. For the most elongated, prolate, spheroids with $e=5$ (see Fig. 1), this closure gives a reasonably accurate representation of the bridge function only at the lower densities $\rho^*\leqslant 0.3$. For $\rho^*=0.4$, which is not far below the isotropic-nematic phase transition, the various components of $b(1,2)$ are very strongly overestimated by the theory. It should be noted that the higher-order components, exemplified here by b_{040}, are harder to determine accurately in the simulation: the feature near $r=0$ in the simulation data may be an artifact of the inversion procedure. For less anisometric shapes, this artifact is much less pronounced.

For the flattest, most oblate, spheroids with $e=\frac{1}{5}$ (see Fig. 2), reasonable agreement between the HCD closure and the simulation results is once more obtained for $\rho^*\leqslant 0.3$, although significant deviations are seen for the b_{000} component even at $\rho^*=0.3$. The closure significantly overestimates the variation in all components for $\rho^*=0.4$. Once more, there is a qualitative difference between simulation and theory for the b_{040} component, particularly at short distances.

For the case of spheroids with $e=3,\frac{1}{3},2,\frac{1}{2}$ (see Figs. 3–6), the HCD closure gives a reasonably accurate representation of the bridge function components up to reduced density $\rho^*=0.5$; at $\rho^*=0.6$, significant differences appear. The agreement becomes progressively better with increasing sphericity, and is very good for the most nearly spherical cases $e=3/2$ and $e=2/3$ (Figs. 7 and 8).

B. The closure relation

A key aim of this study is to examine the accuracy of the various closure relations, expressed directly as the equation linking $b(1,2)$ with $\gamma(1,2)$. A convenient way to present this is the Duh-Haymet plot [34]: for a wide selection of separations and orientations, the values of $b(1,2)$ and $\gamma(1,2)$ are simply plotted against each other. Results are presented here by reduced density (packing fraction). The prolate and oblate cases are presented separately for clarity, but otherwise the

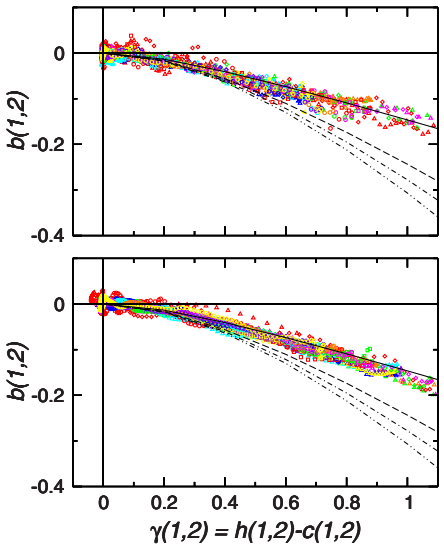

FIG. 9. (Color online) Duh-Haymet plot of bridge function $b(1,2)$ versus indirect correlation function $\gamma(1,2)=h(1,2)-c(1,2)$, determined by Monte Carlo simulation, at reduced density $\rho^*=0.1$. The results of all elongations, eight mutual orientations, and a regular sample of all center-center separations, are superimposed. Orientations defined in Table I: e, s, t, x, a, b, c, d (red, green, blue, cyan, magenta, orange, violet, yellow, respectively). Prolate elongations are shown in the upper graph, oblate elongations in the lower graph: $e=5$, 1/5 (triangles); 3, 1/3 (diamonds); 2, 1/2 (squares); 3/2, 2/3 (circles). Theoretical closure relations are indicated by lines: Henderson-Chan-Degrève [27,28], solid line; modified Verlet [19,23], dashed line; Verlet bridge [26], dot-dashed line; Percus-Yevick, double-dot-dashed line.

results for various elongations, all the mutual orientations listed in Table I, and a regular sampling of all the center-center distances, are superimposed on one another. This allows a test of the possible universality of the various closure relations given in Sec. II: the Duh-Haymet plots are predicted to be identical for equal packing fractions. As will become apparent, although the general form of the plots is the same, there is a clear dependence on packing fraction, which is best represented by the HCD closure.

At the lowest reduced density $\rho^*=0.1$ (see Fig. 9) the HCD closure is very accurate, while the others are not as good. The first term in the expression for α in Eq. (4) was chosen to give a very good approximation for the low-density hard-sphere bridge function, and this term dictates the low-density behavior of the closure relation.

At $\rho^*=0.2$ (see Fig. 10) the HCD closure is still very accurate. There is a small systematic spread in the MC results: for prolate shapes in particular they lie slightly above the HCD line.

At $\rho^*=0.3$ (see Fig. 11) the HCD closure accurately represents all the MC results, except those for the cases $e=5,\frac{1}{5}$ which lie somewhat above the HCD line. As the density increases, the MV closure starts to approach the HCD line from below, but at $\rho^*=0.3$, this and the other closures are clearly worse.

At $\rho^*=0.4$ (see Fig. 12) the MC results do not collapse so well onto a single curve. The most prolate case $e=5$ gives a

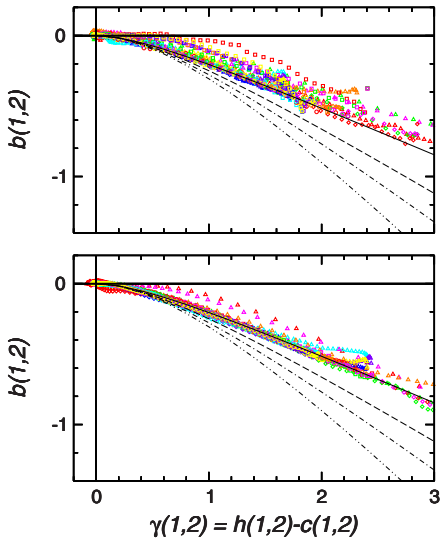

FIG. 10. (Color online) Duh-Haymet plot of bridge function $b(1,2)$ versus indirect correlation function $\gamma(1,2)=h(1,2)-c(1,2)$, determined by Monte Carlo simulation, at reduced density $\rho^*=0.2$. The results of all elongations (prolate above, oblate below), eight mutual orientations, and a regular sample of all center-center separations are superimposed. Theoretical closure relations are indicated by lines. Notation as for Fig. 9.

set of data points lying significantly above the HCD line; for $e=3$, the results lie slightly above the line. For the other elongations, the HCD closure and the MV closure, which almost coincides with it, are very accurate. For $e=\frac{1}{5}$ there is considerable variation in the curves for different orientations.

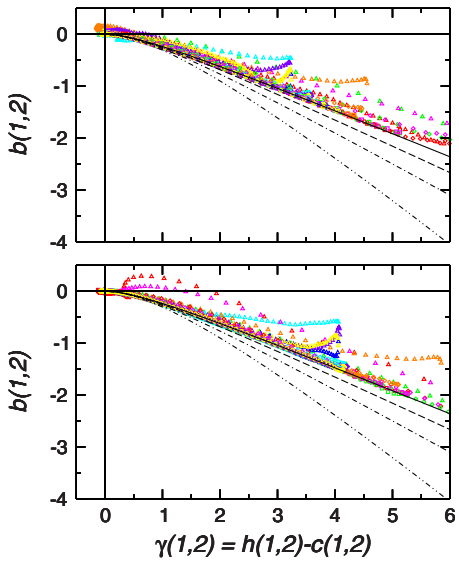

FIG. 11. (Color online) Duh-Haymet plot of bridge function $b(1,2)$ versus indirect correlation function $\gamma(1,2)=h(1,2)-c(1,2)$, determined by Monte Carlo simulation, at reduced density $\rho^*=0.3$. The results of all elongations (prolate above, oblate below), eight mutual orientations, and a regular sample of all center-center separations are superimposed. Theoretical closure relations are indicated by lines. Notation as for Fig. 9.

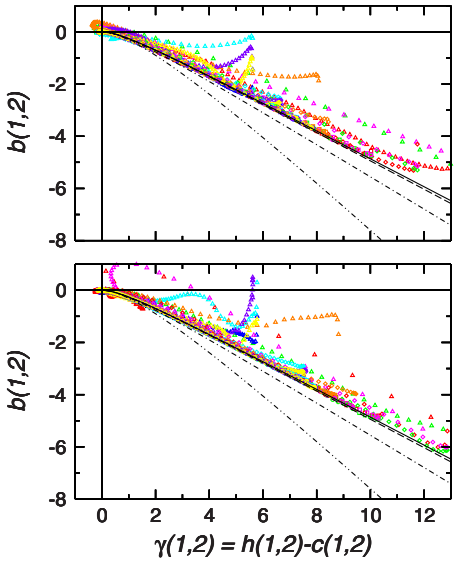

FIG. 12. (Color online) Duh-Haymet plot of bridge function $b(1,2)$ versus indirect correlation function $\gamma(1,2)=h(1,2)-c(1,2)$, determined by Monte Carlo simulation, at reduced density $\rho^*=0.4$. The results of all elongations (prolate above, oblate below), eight mutual orientations, and a regular sample of all center-center separations are superimposed. Theoretical closure relations are indicated by lines. Notation as for Fig. 9.

The cases $e=5,\frac{1}{5}$ are not studied at higher densities, due to the onset of the nematic phase. At $\rho^*=0.5$ (see Fig. 13) both the cases $e=3$ and $1/3$ lie somewhat above the HCD and VB closures, which are almost coincident here. The other elongations fall quite accurately onto the HCD line. At

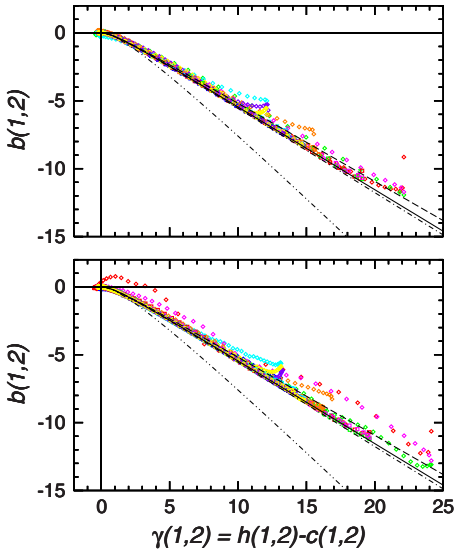

FIG. 13. (Color online) Duh-Haymet plot of bridge function $b(1,2)$ versus indirect correlation function $\gamma(1,2)=h(1,2)-c(1,2)$, determined by Monte Carlo simulation, at reduced density $\rho^*=0.5$. The results of all elongations except $e=5,1/5$ (prolate above, oblate below), eight mutual orientations, and a regular sample of all center-center separations, are superimposed. Theoretical closure relations are indicated by lines. Notation as for Fig. 9.

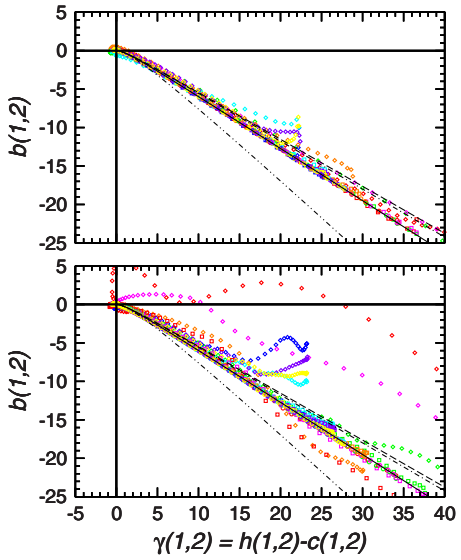

FIG. 14. (Color online) Duh-Haymet plot of bridge function $b(1,2)$ versus indirect correlation function $\gamma(1,2)=h(1,2)-c(1,2)$, determined by Monte Carlo simulation, at reduced density $\rho^*=0.6$. The results of all elongations except $e=5,1/5$ (prolate above, oblate below), eight mutual orientations, and a regular sample of all center-center separations, are superimposed. Theoretical closure relations are indicated by lines. Notation as for Fig. 9.

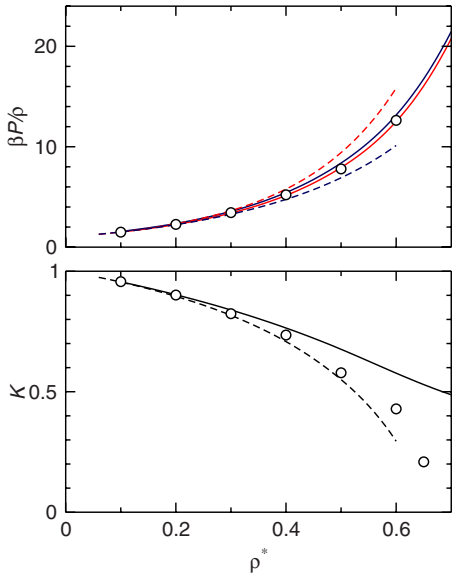

FIG. 15. (Color online) The equation of state (upper panel) obtained via the virial (red, light gray) and compressibility (blue, dark gray) routes and the Kerr coefficient (lower panel) for $e=3$. In both cases, theoretical predictions obtained with HNC equation (dashed lines), HCD Verlet bridge (solid lines), and MC data (circles) are shown.

this density, the MV line lies above all the others.

At the highest density reported here, $\rho^*=0.6$ (see Fig. 14) there is a little more scatter in the MC results. For elongations $e=2,3/2,2/3$, these are accurately represented by the HCD closure. The same is true for $e=1/2$ and $1/3$ at most orientations, but the end-to-end case "e" (better called face to face for these oblate spheroids) lies well off this line. The most prolate elongation $e=3$ conforms reasonably well to the HCD prediction, but there is some scatter. All the elongations have some orientations and positions for which $\gamma(1,2)$ takes small negative values, the case $e=3$ being the most extreme. At this density both MV and VB results lie above the HCD line.

We conclude the discussion with a warning about the accuracy of different closure relations in predicting other structural properties. In Fig. 15 one can see that the gap between the compressibility factor values computed via the virial or the compressibility equations (for the precise definitions see, e.g., Ref. [23]) are significantly reduced and the agreement with MC data is improved when the HCD Verlet bridge function is used in the closure, instead of the simple HNC equation. However Fig. 15 shows that the same does not apply to the value of the Kerr constant, which measures local orientational order (see Ref. [35]). Neither HNC nor HCD closures are in particularly good agreement with the MC data. It remains an open challenge to extend the Verlet bridge function to a form that preserves the small inconsistency for the equation of state and improves the values of the Kerr constant.

V. CONCLUSIONS

Our results show that the closure relations of modified Verlet bridge type are significantly better than both HNC and PY closures of the Ornstein-Zernike equation, for this class of models. Taking the HCD closure as an example, the angular components of the bridge function from Monte Carlo simulation are reasonably well represented up to reduced densities of $\rho^*=0.5$, although there are some discrepancies between the MC and IET data for the higher-order expansion coefficients in the region $r\rightarrow 0$. In investigating the possible "universality" of the closure relation, we find that MC results for the same reduced density or packing fraction do indeed lie very close to the same curve in a Duh-Haymet plot, for a variety of elongations, separations, and relative orientations. This holds, again, up to densities of about $\rho^*=0.5$, beyond which there is a little more scatter, and orientation dependence, although some deviations are seen at lower densities for more anisometric molecules. However, the results also show that this curve is mildly density dependent, and that the HCD closure is the most accurate of those we have tested at all densities.

ACKNOWLEDGMENTS

This work was supported by EPSRC Grants No. GR/S77240 and No. GR/S77103. Computational resources were provided by the Centre for Scientific Computing, University of Warwick and Manchester Computing, University of Manchester.

[1] J.-P. Hansen and I. R. McDonald, *Theory of Simple Liquids*, 2nd ed. (Academic Press, London, 1986).
[2] C. G. Gray and K. E. Gubbins, *Theory of Molecular Fluids. 1. Fundamentals* (Clarendon Press, Oxford, 1984).
[3] R. D. Groot, J. P. van der Eerden, and N. M. Faber, J. Chem. Phys. **87**, 2263 (1987).
[4] G. M. Torrie and G. N. Patey, Mol. Phys. **34**, 1623 (1977).
[5] J. A. Ballance and R. J. Speedy, Mol. Phys. **54**, 1035 (1985).
[6] M. Llanorestrepo and W. G. Chapman, J. Chem. Phys. **97**, 2046 (1992).
[7] M. Llanorestrepo and W. G. Chapman, J. Chem. Phys. **100**, 5139 (1994).
[8] J. Kolafa, S. Labík, and A. Malíjevsky, Mol. Phys. **100**, 2629 (2002).
[9] F. J. Rogers and D. A. Young, Phys. Rev. A **30**, 999 (1984).
[10] G. Zerah and J.-P. Hansen, J. Chem. Phys. **84**, 2336 (1986).
[11] Y. Rosenfeld and N. W. Ashcroft, Phys. Rev. A **20**, 1208 (1979).
[12] P. Attard and G. N. Patey, J. Chem. Phys. **92**, 4970 (1990).
[13] S. Rast, P. H. Fries, and H. Krienke, Mol. Phys. **96**, 1543 (1999).
[14] P. H. Fries and G. N. Patey, J. Chem. Phys. **82**, 429 (1985).
[15] A. Perera, P. G. Kusalik, and G. N. Patey, J. Chem. Phys. **87**, 1295 (1987).
[16] A. Perera and G. N. Patey, J. Chem. Phys. **89**, 5861 (1988).
[17] M. Letz and A. Latz, Phys. Rev. E **60**, 5865 (1999).
[18] R. C. Singh, J. Ram, and Y. Singh, Phys. Rev. E **54**, 977 (1996).
[19] S. Labík, A. Malijevský, and W. R. Smith, Mol. Phys. **73**, 87 (1991).
[20] S. Labík, A. Malijevský, and W. R. Smith, Mol. Phys. **73**, 495 (1991).
[21] R. Pospísil, A. Malijevský, S. Labík, and W. R. Smith, Mol. Phys. **74**, 253 (1991).
[22] S. Labík, A. Malijevský, R. Pospísil, and W. R. Smith, Mol. Phys. **74**, 261 (1991).
[23] R. Pospísil, A. Malijevský, and W. R. Smith, Mol. Phys. **79**, 1011 (1993).
[24] E. Lomba, M. Lombardero, and J. L. F. Abascal, J. Chem. Phys. **90**, 7330 (1989).
[25] D. L. Cheung, L. Anton, M. P. Allen, and A. J. Masters, Phys. Rev. E **73**, 061204 (2006).
[26] L. Verlet, Mol. Phys. **41**, 183 (1980).
[27] D. Henderson, K. Y. Chan, and L. Degrève, J. Chem. Phys. **101**, 6975 (1994).
[28] D. Henderson, A. Malijevský, S. Labík, and K. Y. Chan, Mol. Phys. **87**, 273 (1996).
[29] L. Blum and A. J. Torruella, J. Chem. Phys. **56**, 303 (1972).
[30] J. Talbot, A. Perera, and G. N. Patey, Mol. Phys. **70**, 285 (1990).
[31] M. Pernice and H. F. Walker, SIAM J. Sci. Comput. (USA) **19**, 302 (1998).
[32] A. Donev, F. H. Stillinger, P. M. Chaikin, and S. Torquato, Phys. Rev. Lett. **92**, 255506 (2004).
[33] P. Pfleiderer and T. Schilling, Phys. Rev. E **75**, 020402(R) (2007).
[34] D.-M. Duh and A. D. J. Haymet, J. Chem. Phys. **97**, 7716 (1992).
[35] J. Stecki and A. Kloczkowski, J. Phys. (Paris) **40**, 360 (1979).